

# Serum Metabolite Signatures of Type 2 Diabetes Mellitus Complications

Tao Wu,<sup>†,‡,§</sup> Guoxiang Xie,<sup>§,||</sup> Yan Ni,<sup>§,||</sup> Tao Liu,<sup>‡</sup> Ming Yang,<sup>‡</sup> Huafeng Wei,<sup>‡</sup> Wei Jia,<sup>\*,§,||</sup> and Guang Ji<sup>\*,‡</sup>

<sup>†</sup>Center of Chinese Medical Therapy and Systems Biology, Shanghai University of Traditional Chinese Medicine, 1200 Cailun Road, Shanghai 201203, China

<sup>‡</sup>Institute of Digestive Disease, Longhua Hospital, Shanghai University of Traditional Chinese Medicine, 725 Wanping Road, Shanghai 200032, China

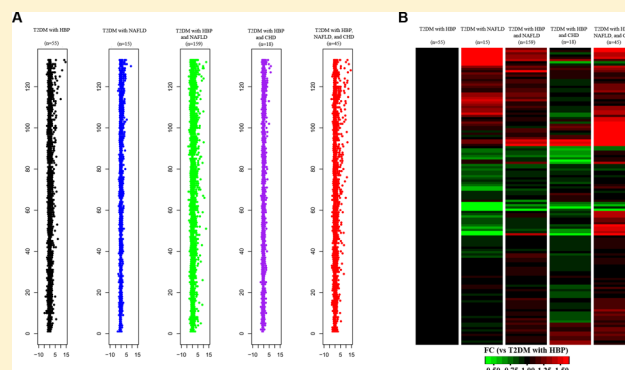
<sup>§</sup>Center for Translational Medicine, and Shanghai Key Laboratory of Diabetes Mellitus, Department of Endocrinology and Metabolism, Shanghai Jiao Tong University Affiliated Sixth People's Hospital, 600 Yishan Road, Shanghai 200233, China

<sup>||</sup>University of Hawaii Cancer Center, 701 Ilalo Street, Honolulu, Hawaii 96813, United States

## Supporting Information

**ABSTRACT:** A number of metabolic conditions, including hypoglycemia, high blood pressure (HBP), dyslipidemia, nerve damage and amputation, and vision problems, occur as a result of uncontrolled blood glucose levels over a prolonged period of time. The different components of diabetic complications are not independent but rather interdependent of each other, rendering the disease difficult to diagnose and control. The underlying pathogenesis of those components cannot be easily elucidated because of the heterogeneous, polygenic, and multifactorial nature of the disease. Metabonomics offers a snapshot of distinct biochemical variations that may reflect the unique metabolic phenotype under pathophysiological conditions. Here we report a mass-spectrometry-based metabolomic study designed to identify the distinct metabolic changes associated with several complications of type 2 diabetes mellitus (T2DM). The 292 patients recruited in the study were divided into five groups, including T2DM with HBP, T2DM with nonalcoholic fatty liver disease (NAFLD), T2DM with HBP and NAFLD, T2DM with HBP and coronary heart disease (CHD), and T2DM with HBP, NAFLD, and CHD. Serum differential metabolites were identified in each group of T2DM complication, mainly involving bile acid, fatty acid, amino acid, lipid, carbohydrate, steroids metabolism, and tricarboxylic acids cycle. These broad-spectrum metabolic changes emphasize the complex abnormalities present among these complications with elevated blood glucose levels, providing a novel strategy for stratifying patients with T2DM complications using blood-based metabolite markers.

**KEYWORDS:** type-2 diabetes mellitus, metabolic signatures, complication, metabolomic profiling, serum



## ■ INTRODUCTION

Metabolic syndrome is defined as a constellation of metabolic disturbances including abdominal obesity, hyperglycemia, hypertension, or high blood pressure (HBP) and dyslipidemia.<sup>1</sup> The different components of metabolic syndrome are not independent but rather interdependent of each other, making the disease rather difficult to diagnose and control.<sup>2</sup> Diabetes mellitus (DM), which affects more than 230 million people worldwide, is often accompanied by cardiovascular disease (CVD) risk factors, such as HBP, dyslipidemia, nonalcoholic fatty liver disease (NAFLD), or coronary heart disease (CHD).<sup>3</sup> At present, these CVD risk factors cannot be clearly identified in routine clinical practice, thus remaining poorly controlled in the DM patients.<sup>4,5</sup> CVD is the major cause of mortality for patients with diabetes and is about two times more frequent in

diabetic patients than those without diabetes.<sup>6</sup> Although the pathogenesis of diabetes is greatly influenced by genetic, lifestyle, and environmental factors, the underlying physiological and metabolic drivers are yet to be fully elucidated. Diabetic complications often represent a challenge in drug treatment, as patients need an individualized therapeutic approach based on their particular health profile. Clinical trials have confirmed a reduction in cardiovascular risk for type 2 DM (T2DM) patients from treatment of dyslipidemia and HBP.<sup>7</sup> Because many patients with diagnosed T2DM may have already been

**Special Issue:** Environmental Impact on Health

**Received:** August 5, 2014

**Published:** September 23, 2014

affected by one or more macro- or microvascular complications, novel biomarkers for stratifying different diabetic complications are critically needed to improve the control of CVD risk factors in the treatment of T2DM.<sup>8</sup>

With the advent of small molecule profiling technology coupled to chemometrics, metabonomics has rapidly become an important approach to measuring an entire spectrum of endogenous metabolites in cells, biofluids, or tissues for mechanistic studies of metabolic diseases.<sup>9–12</sup> There is mounting evidence that metabonomics can provide important insight into the pathogenic nature of various diseases.<sup>13–15</sup> Recently, metabonomics approach has been increasingly applied to biomarker discovery of T2DM,<sup>16–19</sup> HBP,<sup>20</sup> NAFLD,<sup>3,21</sup> and CHD.<sup>22,23</sup> Although a number of metabolic changes have been identified in these diseases, key metabolic pathways mechanistically associated with pathogenesis of diabetes accompanied by different complications are not fully understood. To date, serum metabolite profiles among diabetic patients along with different complications including HBP, NAFLD, and CHD have not been reported. Here we hypothesized that significant metabolic variations may exist in patients with different diabetic complications, and identification of these variations may provide potential clinical biomarkers important for patient stratification and disease prognosis. We conducted a serum metabonomic study on a group of T2DM patients from a population-based cohort study using an ultraperformance liquid chromatography system coupled to a quadrupole-time-of-flight mass spectrometry (UPLC–QTOF/MS), with the goal of identifying characteristic metabolite signatures associated with different complications of T2DM.

## MATERIALS AND METHODS

### Subjects

A total of 292 T2DM subjects were recruited from the Tianlin Community Health Center, Shanghai, China, from August 2009 to May 2010. DM is characterized by a fasting plasma glucose (FPG) of  $\geq 7.0$  mmol/L, 2 h postprandial plasma glucose (2 h PG) of  $\geq 11.1$  mmol/L, or a history of oral hypoglycemic or insulin use, or both, based on the standard formulated by the World Health Organization in 1999.<sup>24</sup> HBP was defined as systolic blood pressure (SBP)  $\geq 140$  mmHg or diastolic blood pressure (DBP)  $\geq 90$  mmHg or use of antihypertensive treatment according to hypertension diagnostic standards from WHO/International Society of Hypertension Committee (WHO/ISH) in 1999.<sup>25</sup> NAFLD was defined according to the definition and treatment guidelines for NAFLD by the Chinese Hepatology Association in 2006.<sup>26</sup> Diagnosis of CHD followed “the Treatment Guide of Stable Angina” (ACC/AHA/ACP-ASIM, 1999) and “Diagnosis and Treatment Recommendations of Unstable Angina” (Chinese Society of Cardiology, 2000).<sup>27,28</sup> Exclusion criteria include alcohol intake of more than 20 g/day, with positive tests indicating the presence of hepatitis B or C virus or toxic liver disease. Moreover, those who had psychiatric disorders or were mentally or intellectually challenged were also excluded. Ethical approval for the study was obtained, and the study was performed in accordance with the principles contained in the Declaration of Helsinki. All participants provided written informed consent prior to the study.

### Chemicals and Reagents

All of the mammalian metabolite standards used for compound annotation and L-chlorophenylalanine used as internal standard for quality control were purchased from Sigma Aldrich

(St. Louis, MO). Formic acid, methanol, and acetonitrile for HPLC grade were purchased from Merck Chemicals (Darmstadt, Germany). All aqueous solutions were prepared with ultrapure water produced by a Milli-Q water purification system (Millipore, Billerica, MA).

### Biochemical Measurements

Body mass index (BMI), waist circumference (WC), hip circumference (HC), waist–hip ratio (WHR), SBP, DBP, FPG, 2h PG, triglyceride (TG), high density lipoprotein (HDL-C), very low-density lipoprotein cholesterol (VLDL-C), and alanine aminotransferase (ALT) were measured as previously described.<sup>18</sup>

### Serum Sample Preparation

Serum samples were collected in the morning before breakfast and stored at  $-80^{\circ}\text{C}$  until UPLC–QTOFMS analysis. Following our previous procedure,<sup>13</sup> a 100  $\mu\text{L}$  aliquot of serum sample was spiked with an internal standard (100  $\mu\text{L}$  L-chlorophenylalanine in water, 0.1 mg/mL). The mixed solution was extracted with 400  $\mu\text{L}$  of methanol and acetonitrile (5:3) and vortexed for 2 min. The mixture was kept at room temperature for 10 min and then centrifuged at 14 500 g for 20 min. The resulting supernatants were transferred into the sampling vial for UPLC–QTOFMS analysis.

### UPLC–QTOFMS Spectral Acquisition of Serum Samples

A 5  $\mu\text{L}$  aliquot of the supernatant was injected into a 100 mm  $\times$  2.1 mm, 1.7  $\mu\text{m}$  BEH C18 column (Waters, Milford, MA) maintained at  $50^{\circ}\text{C}$  using a UPLC system equipped with a binary solvent manager and a sample manager coupled to a QTOF mass spectrometry with an electrospray ion source (Waters, Milford, MA) with the same procedure previously used.<sup>13</sup> The binary gradient elution system consisted of water with 0.1% v/v formic acid (A) and acetonitrile with 0.1% v/v formic acid (B) for positive ion mode (ES+) and water (A) and acetonitrile (B) for negative ion mode (ES–). The separation was achieved using the following gradient: 1–20% B over 0–1 min, 20–70% B over 1–3 min, 70–85% B over 3–8 min, 85–100% B over 8–9 min, and 100% B for 0.5 min with a flow rate of 0.4 mL/min. The source temperature was set to  $120^{\circ}\text{C}$ , and a desolvation gas temperature was set to  $300^{\circ}\text{C}$  with a gas flow of 600 L/h. In the positive and negative ion modes, the capillary voltage was set to 3.2 and 3 kV, and the cone voltage was set to 35 and 50 V, respectively. Centroid data were collected for each sample from 50 to 1000  $m/z$  with a scan time of 0.3 s and interscan delay of 0.02 s over a 5 min analysis time.

### Data Pretreatment and Data Analysis

The acquired UPLC–QTOFMS ES+ and ES– raw data were analyzed by the MarkerLynx Applications Manager 4.1 (Waters, Manchester, U.K.) using parameters reported in our previous work.<sup>13,29</sup> After pretreatment including baseline correction, denoising, smoothing, alignment, time-window splitting, and multivariate curve resolution, the resulting 3-D matrix including assigned peak index [retention time (RT)–molecular weight ( $m/z$ ) pairs], sample names, and ion intensity information was obtained. To acquire consistent differential variables, we further reduced the resulting matrix by removing any peaks with missing value (ion intensity = 0) in  $>80\%$  samples. Metabolites with detectable features (defined by a pair of  $m/z$  and RT) were annotated with the aid of our in-house reference standard library and web-based resources, such as the Human Metabolome Database (HMDB, <http://www.hmdb.ca/>). Metabolites

annotated were subjected to further statistical analysis by univariate and multivariate statistical methods.

Data were expressed as mean  $\pm$  standard deviation (S.D.). Class-specific metabolomic patterns were visualized using z-score plots and heat map after mean centering and unit variance scaling with R software (version 2.15.0, [www.r-project.org](http://www.r-project.org)). The corresponding up- and down-regulated trend showed how these selected differential metabolites varied among these five groups. Differential metabolites among groups were identified by use of one-way analysis of variance (ANOVA) with a threshold of  $P < 0.05$  in the SPSS 17.0 software (SPSS, Chicago, IL). Spearman's rank correlation coefficient ( $r_p$ ) was used to assess the correlation between five groups and these differential metabolites. Metabolites with absolute values of  $r_p > 0.250$  and Spearman  $P < 0.05$  were selected. Principal components analysis (PCA) and orthogonal partial least-squares-discriminant analysis (OPLS-DA) were carried out to assess the metabolomic patterns of the five diabetes groups using SIMCA-P 12.0 software (Umetrics, Umeå, Sweden). The altered metabolic pathways between each two groups were analyzed by means of the quantitative enrichment analysis (QEA) algorithm represented in metabolite set enrichment analysis (MSEA) method based on the differential metabolites within each two groups.<sup>30</sup> Visualization of the significantly perturbed metabolic pathways between each two groups was achieved by using MetScape 2 running on cytoscape.<sup>31,32</sup>

## RESULTS

### Demographics and Clinical Characteristics

The distribution of several diabetic complications in a total of 292 T2DM subjects is shown in Figure 1. Patients were divided

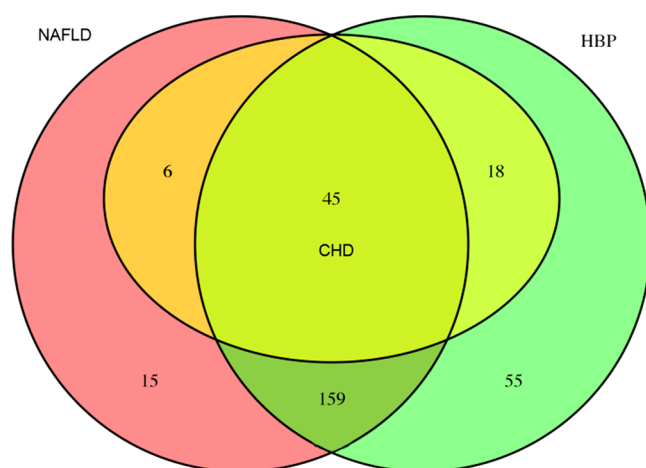


**Figure 1.** Distribution of different complications in T2DM subjects. Venn diagram showed that 292 T2DM subjects were divided into five subgroups. T2DM with HBP ( $n = 55$ ), T2DM with NAFLD ( $n = 15$ ), T2DM with HBP and NAFLD ( $n = 159$ ), T2DM with HBP and CHD ( $n = 18$ ), and T2DM with HBP, NAFLD, and CHD ( $n = 45$ ).

into five subgroups: T2DM with HBP ( $n = 55$ ), T2DM with NAFLD ( $n = 15$ ), T2DM with HBP and NAFLD ( $n = 159$ ), T2DM with HBP and CHD ( $n = 18$ ), and T2DM with HBP, NAFLD, and CHD ( $n = 45$ ).

As shown in Table 1, there were no significant differences in gender, SBP, DBP, FPG, TG, and VLDL among the five study groups based on ANOVA analysis ( $P > 0.05$ ). The age in T2DM with NAFLD was lower than that in T2DM with HBP

and CHD and T2DM with HBP, NAFLD, and CHD ( $P < 0.05$ ). The BMI and WC were significantly higher in T2DM with HBP and NAFLD and T2DM with HBP, NAFLD, and CHD than that in T2DM with HBP ( $P < 0.05$ ), and the level of ALT in T2DM with HBP, NAFLD, and CHD was higher than that in T2DM with HBP and T2DM with HBP and CHD ( $P < 0.05$ ). These differences all indicated that T2DM patients who have more complications would be older and with higher BMI, WC, and ALT. However, other statistical significances between groups were not found.

### Serum Global Metabolic Profiles of T2DM Patients with Different Complications

We have obtained approximately 6680 spectral features of a serum sample after deleting the repeated features and annotated 133 metabolites with our in-house reference standard library and HMDB (Supporting Information Table S1). The metabolic profiles of T2DM patients with different complications were systemically characterized by UPLC-QTOFMS. Global difference was observed among these five groups by using 133 metabolites, as shown in Figure 2. Figure 2A presents the z-score plots of metabolic alterations among five diabetic groups using the ratio of mean rankings. Fold change (FC) of each metabolite was used to construct a heat map, visualizing the changes of these metabolites in different groups as compared with T2DM with HBP groups (Figure 2B). Shades of green and red represent fold decrease or increase of a metabolite, respectively, in T2DM with NAFLD, T2DM with HBP and NAFLD, T2DM with HBP and CHD, or T2DM with HBP, NAFLD, and CHD, relative to T2DM with HBP. PCA and OPLSDA models were carried out to visualize the metabolic difference among each two groups. From the OPLSDA plots, each of the two groups could be separated clearly. The high values of  $R^2X$ ,  $R^2Y$ , and  $Q^2Y$  indicated that these models had good ability of explaining and predicting the metabolic variations between two groups (Figures S1–S10 in the Supporting Information).

### Serum Differential Metabolites among T2DM Patients with Different Complications

Each z-score plot presented metabolic alterations of differential metabolites from the comparison between each two groups according to ANOVA analysis as shown in Figures S11–20 and Table S2 in the Supporting Information. MSEA revealed altered metabolic pathways among each two groups, and visualization of metabolism pathway was performed with cytoscape software. Details were shown in Figures S21–S30 in the Supporting Information. A total of 60 metabolites associated with bile acid metabolism, amino acid metabolism, fatty acid metabolism, lipid metabolism, carbohydrate metabolism, steroids metabolism, and tricarboxylic acids (TCA) cycle were altered including amino acids, steroids, carbohydrates, fatty acids, peptides, nucleosides, organic acids, lipids, and others.

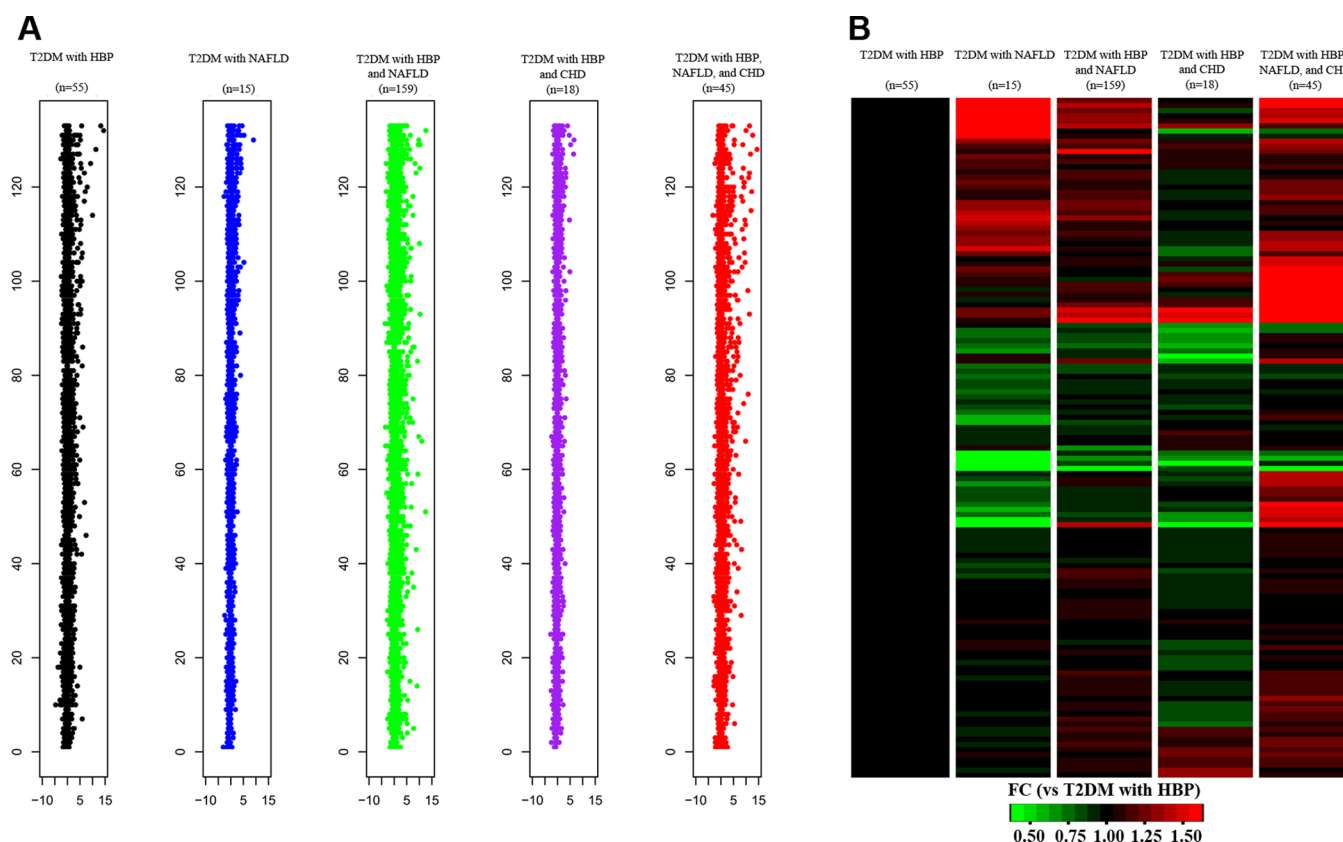
To sift out the metabolites with the most important contribution to different disease phenotypes from ANOVA analysis, we performed a Spearman correlation analysis, and a total of 11 metabolites among the above 60 metabolites were differentially expressed among these five groups based on both correlation coefficient (absolute value of  $r_p > 0.250$ ) and Spearman  $P$  ( $< 0.05$ ) (Table 2). Nine metabolites including taurochenodeoxycholic acid (TCDC), estrone glucuronide, *n*-decanoic acid, 12 $\alpha$ -hydroxy-3-oxocholadienic acid, serine, 3,4,5-trimethoxycinnamic acid, glycocholic acid (GCA), 2-methylcitric acid, and 4-hydroxy tolbutamide were positively correlated with groups.



Table 1. Clinical and Biological Characteristics in T2DM Subjects with Different Complications<sup>a</sup>

variable	T2DM with HBP	T2DM with NAFLD	T2DM with HBP and NAFLD	T2DM with HBP and CHD	T2DM with HBP, NAFLD, and CHD
N (male/female)	26/29	7/8	58/101	6/12	10/35
age (years)	69.78 ± 10.87	62.53 ± 11.72	70.23 ± 8.48	74.17 ± 8.35 <sup>b</sup>	72.84 ± 7.06 <sup>b</sup>
BMI (kg/m <sup>2</sup> )	23.76 ± 2.14	24.26 ± 3.38	25.69 ± 2.88 <sup>aa</sup>	23.95 ± 1.77 <sup>c</sup>	26.55 ± 3.21 <sup>aa,dd</sup>
WC (cm)	88.39 ± 5.76	89.60 ± 7.13	91.46 ± 8.50 <sup>a</sup>	86.44 ± 4.51 <sup>cc</sup>	93.54 ± 8.15 <sup>aa,dd</sup>
HC (cm)	98.86 ± 6.10	97.07 ± 6.96	101.69 ± 7.61	99.50 ± 6.51	103.27 ± 8.13 <sup>a</sup>
WHR	0.89 ± 0.05	0.92 ± 0.05	0.90 ± 0.05	0.87 ± 0.05	0.91 ± 0.06
SBP (mmHg)	137.53 ± 13.02	132.27 ± 11.80	139.46 ± 14.46	138.22 ± 19.81	138.18 ± 14.29
DBP (mmHg)	76.65 ± 9.93	76.67 ± 7.28	79.47 ± 9.47	77.56 ± 10.82	78.27 ± 9.24
FPG (mmol/L)	7.17 ± 1.94	8.48 ± 2.67 <sup>a</sup>	7.69 ± 2.19	7.06 ± 1.53	7.74 ± 2.18
2hPG (mmol/L)	10.17 ± 3.54	13.04 ± 4.06	11.84 ± 3.63	10.26 ± 2.77	10.83 ± 3.69
TG (mmol/L)	1.34 ± 0.63	1.76 ± 1.07	1.60 ± 1.06	1.51 ± 0.79	1.71 ± 0.79
HDL-C (mmol/L)	1.35 ± 0.34	1.19 ± 0.31	1.34 ± 0.37	1.34 ± 0.39	1.35 ± 0.36
VLDL (mmol/L)	1.35 ± 0.34	1.19 ± 0.31	1.34 ± 0.37	1.34 ± 0.39	1.35 ± 0.36
ALT (U/L)	23.92 ± 13.48	22.21 ± 9.86	24.34 ± 12.06	23.47 ± 10.61	30.31 ± 16.76 <sup>a,d</sup>

<sup>a</sup>Values are presented as mean ± standard deviation. The superscript letter (a, b, c, and d) indicates significant difference between groups at  $P < 0.05$  comparison with T2DM with HBP, T2DM with NAFLD, T2DM with HBP and NAFLD, T2DM with HBP and CHD, respectively, according to ANOVA analysis. If  $P < 0.01$ , the letter doubled. Abbreviations: BMI, body mass index; WC, waist circumference; HC, hip circumference waist; WHR, waist-hip ratio; SBP, systolic blood pressure; DBP, diastolic blood pressure; FPG, fasting plasma glucose; 2hPG, 2h postprandial plasma glucose; HDL-C, high density lipoprotein cholesterol; VLDL-C, very low density lipoprotein; ALT, aspartate aminotransferase.



**Figure 2.** Metabolite signatures of five groups. (A) z-score plots of metabolonomic alterations from different complications of T2DM. Each point represents one metabolite in one sample, colored by type (black = T2DM with HBP, blue = T2DM with NAFLD, green = T2DM with HBP and NAFLD, purple = T2DM with HBP and CHD, red = T2DM with HBP, NAFLD, and CHD). (B) Heat map showing the fold change (FC) of 133 metabolites among five groups compared with T2DM with HBP. Shades of green and red represent fold decrease or increase of a metabolite, respectively, in T2DM with NAFLD, T2DM with HBP and NAFLD, T2DM with HBP and CHD, or T2DM with HBP, NAFLD, and CHD, relative to T2DM with HBP (see color scale).

However, the remaining two metabolites including *n*-dodecanoic acid and androsterone sulfate were negatively correlated with groups. According to the Kyoto Encyclopedia of Genes and Genomes (KEGG) database, several key metabolic

pathways that were altered in T2DM patients with different complications were identified, which involved bile acid metabolism, fatty acid metabolism, and TCA cycle based on the above metabolites (Table 2). To further test the performance

Table 2. Differential Serum Metabolites Between T2DM Subjects with Different Complications

metabolites	metabolic pathway	$r_p^a$	$p^b$	$p^c$	T2DM with HBP	T2DM with NAFLD	T2DM with HBP and NAFLD	T2DM with HBP, NAFLD, and CHD
taurochenodeoxycholic acid	bile acid metabolism	0.47	<0.001	<0.001	32.61 ± 11.99	34.47 ± 15.07	47.52 ± 33.45 <sup>aa</sup>	89.64 ± 124.96 <sup>a</sup>
estrone glucuronide	steroids	0.432	<0.001	<0.001	0.20 ± 0.09	0.19 ± 0.03	0.22 ± 0.06	0.32 ± 0.14 <sup>aabb,cc,dd</sup>
<i>n</i> -dodecanoic acid	fatty acid metabolism	-0.426	<0.001	<0.001	2.14 ± 0.94	2.72 ± 1.37	2.17 ± 1.11 <sup>aa</sup>	2.87 ± 2.34 <sup>abbc</sup>
<i>n</i> -decanoic acid	fatty acid metabolism	0.401	<0.001	0.001	0.32 ± 0.07	0.31 ± 0.06	0.35 ± 0.08	0.39 ± 0.11 <sup>aabb,cc</sup>
12 $\alpha$ -hydroxy-3-oxocholadienic acid	bile acid metabolism	0.394	<0.001	0.012	27.55 ± 7.16	25.55 ± 7.82	30.68 ± 10.16 <sup>bb</sup>	32.93 ± 8.25 <sup>aabb</sup>
3,4,5-trimethoxycinnamic acid	aromatic homomonocyclic compounds	0.343	<0.001	<0.001	0.24 ± 0.06	0.24 ± 0.04	0.25 ± 0.04	0.27 ± 0.04 <sup>aabb,cc,dd</sup>
glycocholic acid	bile acid metabolism	0.328	<0.001	0.001	25.01 ± 7.45	30.21 ± 16.27	34.2 ± 26.87 <sup>aa</sup>	41.38 ± 39.47 <sup>aa</sup>
serine	glycine, serine, methionine, sphingolipid metabolism	0.321	<0.001	0.005	19.21 ± 11.86	14.71 ± 2.02	20.61 ± 9.81	25.35 ± 14.82 <sup>bb,cc,dd</sup>
2-methylcitric acid	TCA cycle	0.293	<0.001	<0.001	0.46 ± 0.19	0.50 ± 0.14	0.42 ± 0.09	0.71 ± 0.41 <sup>aabb,cc,dd</sup>
androsterone sulfate	steroids	-0.288	<0.001	0.002	2.96 ± 1.63	4.96 ± 5.54	2.9 ± 2.09	2.42 ± 2.43 <sup>aabb,cc,dd</sup>
4-hydroxy tolbutamide	aromatic homomonocyclic compounds	0.259	<0.001	0.001	22.44 ± 9.20	36.4 ± 20.09 <sup>aa</sup>	30.65 ± 13.49 <sup>aa</sup>	34.32 ± 27.39 <sup>aa,ad</sup>

<sup>a</sup>Correlation coefficient ( $r_p$ ) was obtained from Spearman correlation analysis with a threshold of absolute value 0.250. <sup>b</sup> $p$  values were calculated from Spearman correlation analysis. <sup>c</sup> $p$  values were from ANOVA analysis. The superscript letter (a, b, c, and d) indicates significant difference between groups at  $P < 0.05$  comparison with T2DM with HBP, T2DM with NAFLD, T2DM with HBP and NAFLD, and T2DM with HBP and CHD, respectively. If  $P < 0.01$ , the letter doubled.

of the selected metabolites, we selected five groups as training samples. A cross-validated OPLS-DA model was constructed based on the 11 differential metabolites, showing a trend of separation among the five subgroups (R2X cum = 0.443, R2Y cum = 0.334, Q2Y cum = 0.268, Figure 3). This result indicated great potential for stratification of diabetes with different complications using these serum metabolite markers.

Furthermore, we deleted the overlapped differential metabolites between groups, and then 16 differential metabolites associated with amino acid, fatty acid, lipid, carbohydrate, steroids metabolism, and TCA cycle were found with specific difference within groups, as illustrated in Figure 4. Heat map showed the fold change of 16 metabolites among five groups in Figure S31 in the Supporting Information. In brief, T2DM with HBP and NAFLD showed higher serum levels of prolyl-proline, dihydroxyfumaric acid, docosahexaenoic acid (DHA), and hypoxanthine than T2DM with HBP. However, serum level of selenocystine in T2DM with HBP and CHD was higher than T2DM with NAFLD, significantly lower stearyl carnitine and leucine compared with T2DM with HBP and NAFLD. T2DM with HBP, NAFLD, and CHD had higher serum levels of elaidic acid than T2DM with HBP, higher xanthine and lower aldosterone than T2DM with NAFLD, higher 4-hydroxy-3-methoxy mandelic acid (VMA) than T2DM with HBP and NAFLD, and higher proline, uridine, *cis*-2-methyl aconitic acid, and cytidine than T2DM with HBP and CHD, respectively. The metabolite levels of pipecolic acid in T2DM with NAFLD were higher than that in T2DM with HBP.

## DISCUSSION

In the present study, we applied a comprehensive metabolomics approach to understand the metabolic differences among different complications of T2DM subjects and how those metabolic profiles were impacted when T2DM were accompanied by one or two or three complications.

On the basis of Spearman correlation analysis, 11 metabolites were correlated with different complications (Table 2). With the growing numbers of complication in T2DM patients, the serum level of TCDCA, GCA, and 12 $\alpha$ -hydroxy-3-oxocholadienic acid belonging to bile acid metabolism increased. Similarly, *n*-decanoic acid of fatty acid metabolism, 2-methylcitric acid of TCA cycle, estrone glucuronide of steroids metabolism, serine of serine metabolism, and 3,4,5-trimethoxycinnamic acid were also found at increased levels in subjects with more than one T2DM complication. However, *n*-dodecanoic acid of fatty acid metabolism and androsterone sulfate of steroids metabolism were decreased in T2DM along with one, two, or three complications. It is noteworthy that serum levels of TCDCA and estrone glucuronide in T2DM with HBP, NAFLD, and CHD were higher than those in any other group with  $r_p$  of 0.470 and 0.432, respectively, suggesting that these two metabolite markers can be potentially used to monitor the development and progression of T2DM complications. Interestingly, T2DM with NAFLD was characterized with higher serum levels of androsterone sulfate and 4-hydroxy tolbutamide than other groups. These results may provide new insights into the underlying pathophysiological mechanisms for the development and progression of metabolic diseases with complications. Furthermore, an OPLS-DA model indicated that the five different groups showed a trend of separation with a panel of the 11 metabolite markers. The above results suggest that we can successfully identify and characterize the delicate differences

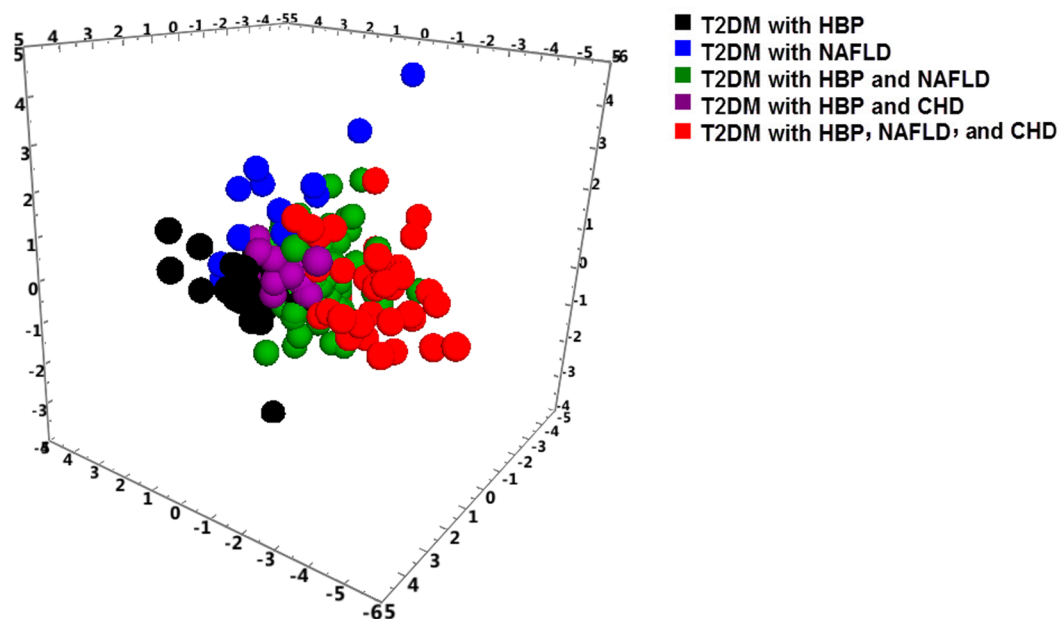


**Figure 3.** Scores plot of the OPLS-DA model in five groups based on 11 detected differential serum metabolites. There is a trend of separation among five groups from the OPLS-DA scores plot based on the 11 differential metabolites. Black = T2DM with HBP, blue = T2DM with NAFLD, green = T2DM with HBP and NAFLD, purple = T2DM with HBP and CHD, red = T2DM with HBP, NAFLD, and CHD.

among T2DM subjects with different complications using a metabonomic profiling approach.

The specific differences within groups are briefly discussed in the following. T2DM with HBP group was used as a baseline when comparing among T2DM complications consisting of HBP alone, and/or NAFLD, and/or CHD. The metabolite profiles of T2DM with HBP and NAFLD were compared with the groups of T2DM with HBP and T2DM with NAFLD, respectively; subsequently two panels of differential metabolites were obtained (Figures S11 and S12 in the Supporting Information). Our results showed that T2DM with HBP and NAFLD had higher prolyl-proline, dihydroxyfumaric acid, DHA, and hypoxanthine than T2DM with HBP specifically (Figure 4). It was reported that tripeptides isoleucyl-prolyl-proline (IPP) and valyl-prolyl-proline (VPP) act as angiotensin-I-converting enzyme inhibitors *in vitro*.<sup>24</sup> Dihydroxyfumaric acid with insulin inhibitory effect is known to generate superoxide anions and hydroxyl free radicals.<sup>33</sup> DHA is an essential component of n3 polyunsaturated fatty acids that may have a role in preventing cardiovascular events and inflammation.<sup>34</sup> DHA could modulate hepatic progenitor cell activation, hepatocyte survival, and macrophage polarization.<sup>35</sup> This metabolite is also found to be able to attenuate hepatic inflammation, oxidative stress, and the development of liver fibrosis without decreasing hepatosteatosis in a mouse model of western diet-induced nonalcoholic steatohepatitis.<sup>36</sup> Hypoxanthine is normally found at low concentrations in human plasma resulting from dietary and endogenous purine metabolism. Rodrigues et al. suggest that hypoxanthine alters antioxidant defenses and induces lipid peroxidation in the kidney of rats.<sup>37</sup> The metabolite profiles in T2DM with HBP and NAFLD are indicative of a more abnormal lipid metabolism than in T2DM with HBP.

The metabolite profiles of T2DM with HBP and CHD were compared with those of T2DM with HBP, T2DM with NAFLD, and T2DM with HBP and NAFLD, respectively; subsequently, three panels of differential metabolites were obtained (Figures S13–S15 in the Supporting Information). Briefly,

compared with T2DM with NAFLD, the serum level of selenocystine was higher in T2DM with HBP and CHD. However, the concentrations of several metabolites were significantly lower in T2DM with HBP and CHD than in T2DM with HBP and NAFLD, including stearoyl carnitine and leucine (Figure 4).

Selenocysteine is a naturally occurring selenoamino acid that exhibits broad-spectrum antiproliferative activity against several human tumor cells through oxidative stress-mediated apoptosis,<sup>38</sup> but its role in the progress of T2DM with HBP and CHD and T2DM with NAFLD is unclear.

Recent studies suggest that at least some of the substrate palmitoyl-CoA and product stearoyl-CoA of the chain elongation have ready access to carnitine palmitoyltransferase and is indicative of alteration in a mitochondrial fatty acid chain elongation pathway.<sup>39</sup> Incomplete fatty acid oxidation results elevated acylcarnitine concentrations.<sup>40</sup> Leucine is one of the branched chain amino acids, and its supplementation has been shown to prevent high-fat diet-induced obesity, hyperglycemia, and dyslipidemia in animal models.<sup>41</sup> Recently, several studies have shown that dietary manipulation of essential amino acids, including leucine, arginine, and glutamine, improves lipid and glucose metabolism.<sup>42</sup> These metabolites were at higher levels in T2DM with HBP and NAFLD with more abnormal lipid metabolism than in T2DM with HBP and CHD.

The metabolite profiles of T2DM with HBP, NAFLD, and CHD were also compared with those of T2DM with HBP, T2DM with NAFLD, T2DM with HBP and NAFLD, and T2DM with HBP and CHD, respectively, and subsequently four panels of differential metabolites were obtained (Figures S16–S19 in the Supporting Information). The results showed that T2DM patients with HBP, NAFLD, and CHD had higher serum levels of GCA and elaidic acid than T2DM with HBP, higher xanthine and lower aldosterone than T2DM with NAFLD, higher VMA than T2DM with HBP and NAFLD, and higher proline, uridine, *cis*-2-methyl aconitic acid, and cytidine than T2DM with HBP and CHD, respectively (Figure 4).

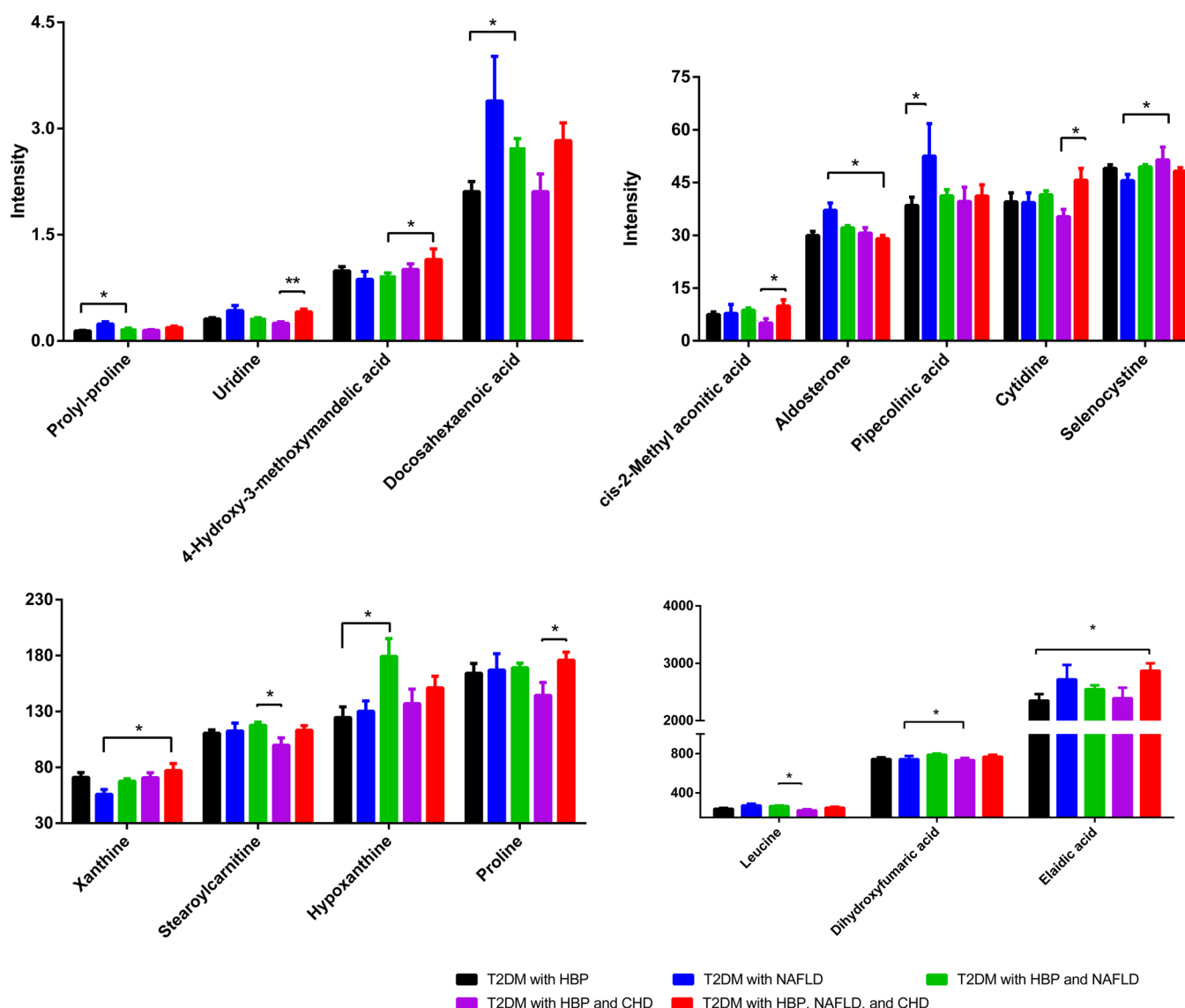


**Figure 4.** Differential metabolites among five groups. Histogram showed 16 differential metabolites in different complications of T2DM ( $P < 0.05$ ). Values are mean intensities  $\pm$  SEM measured using UPLC-QTOFMS. Black = T2DM with HBP, blue = T2DM with NAFLD, green = T2DM with HBP and NAFLD, purple = T2DM with HBP and CHD, red = T2DM with HBP, NAFLD, and CHD. \* presents  $P < 0.05$ ; \*\* presents  $P < 0.01$ .

Elaidic acid, the trans isomer of oleic acid, demonstrated a unique role in modulating hepatic lipogenesis.<sup>43</sup> The results suggest a role of elaidic acid in the progress from T2DM with HBP to T2DM with HBP, NAFLD, and CHD.

Xanthine is an intermediate in the degradation of adenosine monophosphate to uric acid, being formed by oxidation of hypoxanthine. A potential role of uric acid in the pathogenesis of CVD has drawn much attention in recent years,<sup>44,45</sup> suggesting that the higher levels of xanthine may contribute to the development of CHD phenotype. The level of aldosterone was lower in T2DM with HBP, NAFLD, and CHD than in T2DM with NAFLD, which was indicative of more serious imbalance of steroids in T2DM with more complications involved.

VMA, vanillylmandelate, is one of the products of the catabolism of catecholamines (epinephrine, norepinephrine, and dopamine). It was lower in the group of T2DM with HBP and NAFLD than in the group of T2DM with HBP, NAFLD, and CHD, indicating the down-regulated catabolic pathways of the catecholamines. VMA was found to decrease heart rate in a dose-dependent way when administered intra-arterially.<sup>46</sup> Such

a cardiovascular effect of VMA was mediated by increased vagal tone, without  $\alpha$ - or  $\beta$ -adrenergic-receptor blocking activities.<sup>46</sup> This pharmacological evidence along with insignificant correlation coefficients between the serum catecholamine levels and resting systolic and diastolic blood pressure values suggests that elevation in serum concentrations of catecholamine end metabolites is more likely a common metabolic consequence than a possible active role of these metabolites in the pathogenesis of hypertension.

Proline is a nonessential amino acid that is synthesized from glutamic acid as well as an essential component of collagen.<sup>47</sup> Uridine, a pyrimidine nucleoside, can modulate liver lipid metabolism, although its specific targets have not been identified. Uridine has been widely tested in clinical trials for treatments of neurological disorders, liver dysfunction, and cancer.<sup>48</sup> *cis*-2-Methylaconitic acid is produced from the dehydration of 2-methylcitrate in 2-methylcitric acid cycle.<sup>49</sup> Cytidine is a nucleoside composed of the base cytosine linked to the five-carbon sugar D-ribose. It can serve as substrate for the salvage pathway of pyrimidine nucleotide synthesis, a precursor to the cytidine triphosphate needed in the phosphatidylcholine and



phosphatidylethanolamine biosynthetic pathway.<sup>50</sup> These variations may reflect the species differences in cytidine deaminase, the enzyme that converts cytidine to uridine in the body from T2DM with HBP and CHD to T2DM with HBP, NAFLD, and CHD.

Compared with T2DM with HBP, the metabolite profile of T2DM with NAFLD, as depicted in Figure S20 in the Supporting Information, can be characterized by increased level of pipecolic acid (Figure 4). Pipecolic acid is the major metabolic intermediate of lysine. Because pipecolic acid catabolism can produce H<sub>2</sub>O<sub>2</sub> by oxidases,<sup>51</sup> oxidative stress derived from hepatocytes may be a possible mechanism driving the pathophysiological development of T2DM with NAFLD.

## CONCLUSIONS

Our study is the first attempt to stratify different T2DM complications using a metabonomic approach. The results show that a panel of differentially expressed serum metabolites can reflect mechanistic pathways altered among diabetic complications and therefore can be used as a promising screening or stratification method for different T2DM complications. These initial findings provide an improved understanding of the important metabolic alterations associated with T2DM progression, which will be helpful for personalized treatment of diabetic complications in the future.

There are several limitations in the current MS-based metabonomic study. First, the sample size may not be sufficiently large to detect all disease-associated metabolite changes. Second, we were not able to recruit an additional set of T2DM patients without any complications precluding a good control group for the study. Therefore, further investigations with larger sample sizes and patients with early T2DM without complications are needed to confirm our findings.

## ASSOCIATED CONTENT

### Supporting Information

Figure S1. PCA and OPLSDA score plots between T2DM with HBP and T2DM with HBP and NAFLD based on 133 metabolites. Figure S2. PCA and OPLSDA score plots between T2DM with NAFLD and T2DM with HBP and NAFLD based on 133 metabolites. Figure S3. PCA and OPLSDA score plots between T2DM with HBP and T2DM with HBP and CHD based on 133 metabolites. Figure S4. PCA and OPLSDA score plots between T2DM with NAFLD and T2DM with HBP and CHD based on 133 metabolites. Figure S5. PCA and OPLSDA score plots between T2DM with HBP and NAFLD and T2DM with HBP and CHD based on 133 metabolites. Figure S6. PCA and OPLSDA score plots between T2DM with HBP and T2DM with HBP, NAFLD, and CHD based on 133 metabolites. Figure S7. PCA and OPLSDA score plots between T2DM with NAFLD and T2DM with HBP, NAFLD, and CHD based on 133 metabolites. Figure S8. PCA and OPLSDA score plots between T2DM with HBP and NAFLD and T2DM with HBP, NAFLD, and CHD based on 133 metabolites. Figure S9. PCA and OPLSDA score plots between T2DM with HBP and CHD and T2DM with HBP, NAFLD, and CHD based on 133 metabolites. Figure S10. PCA and OPLSDA score plots between T2DM with HBP and T2DM with NAFLD based on 133 metabolites. Figure S11. Differential metabolites between T2DM with HBP and T2DM with HBP and NAFLD. Figure S12. Differential metabolites between T2DM with NAFLD and T2DM with HBP and NAFLD. Figure S13.

Differential metabolites between T2DM with HBP and T2DM with HBP and CHD. Figure S14. Differential metabolites between T2DM with NAFLD and T2DM with HBP and CHD. Figure S15. Differential metabolites between T2DM with HBP and NAFLD and T2DM with HBP and CHD. Figure S16. Differential metabolites between T2DM with HBP and T2DM with HBP, NAFLD, and CHD. Figure S17. Differential metabolites between T2DM with NAFLD and T2DM with HBP, NAFLD, and CHD. Figure S18. Differential metabolites between T2DM with HBP and NAFLD and T2DM with HBP, NAFLD, and CHD. Figure S19. Differential metabolites between T2DM with HBP and CHD and T2DM with HBP, NAFLD, and CHD. Figure S20. Differential metabolites between T2DM with HBP and T2DM with NAFLD. Figure S21. Altered metabolic pathways between T2DM with HBP and T2DM with HBP and NAFLD. Figure S22. Altered metabolic pathways between T2DM with NAFLD and T2DM with HBP and NAFLD. Figure S23. Altered metabolic pathways between T2DM with HBP and T2DM with HBP and CHD. Figure S24. Altered metabolic pathways between T2DM with NAFLD and T2DM with HBP and CHD. Figure S25. Altered metabolic pathways between T2DM with HBP and NAFLD and T2DM with HBP and CHD. Figure S26. Altered metabolic pathways between T2DM with HBP and T2DM with HBP, NAFLD, and CHD. Figure S27. Altered metabolic pathways between T2DM with NAFLD and T2DM with HBP, NAFLD, and CHD. Figure S28. Altered metabolic pathways between T2DM with HBP and NAFLD and T2DM with HBP, NAFLD, and CHD. Figure S29. Altered metabolic pathways between T2DM with HBP and CHD and T2DM with HBP, NAFLD, and CHD. Figure S30. Altered metabolic pathways between T2DM with HBP and T2DM with NAFLD. Figure S31. Heat map showed the fold change of 16 metabolites among five groups. Table S1. Total of 133 representative metabolites derived from UPLC-QTOFMS analysis. Table S2. Total of 60 metabolites with significant differences between groups from ANOVA analysis. This material is available free of charge via the Internet at <http://pubs.acs.org>.

## AUTHOR INFORMATION

### Corresponding Authors

\*W.J.: Tel: 1-808-564-5823. Fax: 1-808-564-2984. E-mail: [wjia@cc.hawaii.edu](mailto:wjia@cc.hawaii.edu).

\*G.J.: Tel: 8621-64286261. Fax: 8621-64286261. E-mail: [jiliver@vip.sina.com](mailto:jiliver@vip.sina.com).

### Notes

The authors declare no competing financial interest.

## ACKNOWLEDGMENTS

This study was financially supported by the National Natural Science Foundation of China (81202979), the Leading Academic Discipline Project and Innovative Research Team in Universities from Shanghai Municipal Education Commission (J50305), and E-institutes of Shanghai Municipal Education Commission China (E03008).

## REFERENCES

- (1) Wang, W. J. Enhancing the treatment of metabolic syndrome with integrative medicine. *J. Integr. Med.* **2013**, *11* (3), 153–156.
- (2) Akilen, R.; Pimlott, Z.; Tsiami, A.; Robinson, N. The use of complementary and alternative medicine by individuals with features of metabolic syndrome. *J. Integr. Med.* **2014**, *12* (3), 171–174.



- (3) Barr, J.; Vazquez-Chantada, M.; Alonso, C.; Perez-Cormenzana, M.; Mayo, R.; Galan, A.; Caballeria, J.; Martin-Duce, A.; Tran, A.; Wagner, C.; Luka, Z.; Lu, S. C.; Castro, A.; Le Marchand-Brustel, Y.; Martinez-Chantar, M. L.; Veyrie, N.; Clement, K.; Tordjman, J.; Gual, P.; Mato, J. M. Liquid chromatography-mass spectrometry-based parallel metabolic profiling of human and mouse model serum reveals putative biomarkers associated with the progression of nonalcoholic fatty liver disease. *J. Proteome Res.* **2010**, *9* (9), 4501–4512.
- (4) Resnick, H. E.; Foster, G. L.; Bardsley, J.; Ratner, R. E. Achievement of American Diabetes Association clinical practice recommendations among U.S. adults with diabetes, 1999–2002: the National Health and Nutrition Examination Survey. *Diabetes Care* **2006**, *29* (3), 531–537.
- (5) Saydah, S. H.; Fradkin, J.; Cowie, C. C. Poor control of risk factors for vascular disease among adults with previously diagnosed diabetes. *JAMA, J. Am. Med. Assoc.* **2004**, *291* (3), 335–342.
- (6) Emerging Risk Factors, C.; Sarwar, N.; Gao, P.; Seshasai, S. R.; Gobin, R.; Kaptoge, S.; Di Angelantonio, E.; Ingelsson, E.; Lawlor, D. A.; Selvin, E.; Stampfer, M.; Stehouwer, C. D.; Lewington, S.; Pennells, L.; Thompson, A.; Sattar, N.; White, I. R.; Ray, K. K.; Danesh, J. Diabetes mellitus, fasting blood glucose concentration, and risk of vascular disease: a collaborative meta-analysis of 102 prospective studies. *Lancet* **2010**, *375* (9733), 2215–2222.
- (7) Chobanian, A. V.; Bakris, G. L.; Black, H. R.; Cushman, W. C.; Green, L. A.; Izzo, J. L., Jr.; Jones, D. W.; Materson, B. J.; Oparil, S.; Wright, J. T., Jr.; Roccella, E. J. The Seventh Report of the Joint National Committee on Prevention, Detection, Evaluation, and Treatment of High Blood Pressure: the JNC 7 report. *JAMA, J. Am. Med. Assoc.* **2003**, *289* (19), 2560–2572.
- (8) McLean, D. L.; McAlister, F. A.; Johnson, J. A.; King, K. M.; Makowsky, M. J.; Jones, C. A.; Tsuyuki, R. T.; Investigators, S.-H. A randomized trial of the effect of community pharmacist and nurse care on improving blood pressure management in patients with diabetes mellitus: study of cardiovascular risk intervention by pharmacists-hypertension (SCRIP-HTN). *Arch. Intern. Med.* **2008**, *168* (21), 2355–2361.
- (9) Suhre, K.; Meisinger, C.; Doring, A.; Altmaier, E.; Belcredi, P.; Gieger, C.; Chang, D.; Milburn, M. V.; Gall, W. E.; Weinberger, K. M.; Mewes, H. W.; Hrahe de Angelis, M.; Wichmann, H. E.; Kronenberg, F.; Adamski, J.; Illig, T. Metabolic footprint of diabetes: a multiplatform metabolomics study in an epidemiological setting. *PLoS One* **2010**, *5* (11), e13953.
- (10) Suhre, K.; Shin, S. Y.; Petersen, A. K.; Mohny, R. P.; Meredith, D.; Wagele, B.; Altmaier, E.; CardioGram; Deloukas, P.; Erdmann, J.; Grundberg, E.; Hammond, C. J.; de Angelis, M. H.; Kastenmuller, G.; Kottgen, A.; Kronenberg, F.; Mangino, M.; Meisinger, C.; Meitinger, T.; Mewes, H. W.; Milburn, M. V.; Prehn, C.; Raffler, J.; Ried, J. S.; Romisch-Margl, W.; Samani, N. J.; Small, K. S.; Wichmann, H. E.; Zhai, G.; Illig, T.; Spector, T. D.; Adamski, J.; Soranzo, N.; Gieger, C. Human metabolic individuality in biomedical and pharmaceutical research. *Nature* **2011**, *477* (7362), 54–60.
- (11) Wang, T. J.; Ngo, D.; Psychogios, N.; Dejam, A.; Larson, M. G.; Vasani, R. S.; Ghorbani, A.; O'Sullivan, J.; Cheng, S.; Rhee, E. P.; Sinha, S.; McCabe, E.; Fox, C. S.; O'Donnell, C. J.; Ho, J. E.; Florez, J. C.; Magnusson, M.; Pierce, K. A.; Souza, A. L.; Yu, Y.; Carter, C.; Light, P. E.; Melander, O.; Clish, C. B.; Gerszten, R. E. 2-Aminoadipic acid is a biomarker for diabetes risk. *J. Clin. Invest.* **2013**, *123* (10), 4309–4317.
- (12) Rhee, E. P.; Cheng, S.; Larson, M. G.; Walford, G. A.; Lewis, G. D.; McCabe, E.; Yang, E.; Farrell, L.; Fox, C. S.; O'Donnell, C. J.; Carr, S. A.; Vasani, R. S.; Florez, J. C.; Clish, C. B.; Wang, T. J.; Gerszten, R. E. Lipid profiling identifies a triacylglycerol signature of insulin resistance and improves diabetes prediction in humans. *J. Clin. Invest.* **2011**, *121* (4), 1402–1411.
- (13) Qiu, Y.; Cai, G.; Su, M.; Chen, T.; Zheng, X.; Xu, Y.; Ni, Y.; Zhao, A.; Xu, L. X.; Cai, S.; Jia, W. Serum metabolite profiling of human colorectal cancer using GC-TOFMS and UPLC-QTOFMS. *J. Proteome Res.* **2009**, *8* (10), 4844–4850.
- (14) Chen, T.; Xie, G.; Wang, X.; Fan, J.; Qiu, Y.; Zheng, X.; Qi, X.; Cao, Y.; Su, M.; Wang, X.; Xu, L. X.; Yen, Y.; Liu, P.; Jia, W. Serum and urine metabolite profiling reveals potential biomarkers of human hepatocellular carcinoma. *Mol. Cell. Proteomics* **2011**, *10* (7), M110 004945.
- (15) Bernini, P.; Bertini, I.; Luchinat, C.; Tenori, L.; Tognaccini, A. The cardiovascular risk of healthy individuals studied by NMR metabolomics of plasma samples. *J. Proteome Res.* **2011**, *10* (11), 4983–4992.
- (16) Connor, S. C.; Hansen, M. K.; Corner, A.; Smith, R. F.; Ryan, T. E. Integration of metabolomics and transcriptomics data to aid biomarker discovery in type 2 diabetes. *Mol. Biosyst.* **2010**, *6* (5), 909–921.
- (17) Huo, T.; Cai, S.; Lu, X.; Sha, Y.; Yu, M.; Li, F. Metabonomic study of biochemical changes in the serum of type 2 diabetes mellitus patients after the treatment of metformin hydrochloride. *J. Pharm. Biomed. Anal.* **2009**, *49* (4), 976–982.
- (18) Wu, T.; Yang, M.; Wei, H. F.; He, S. H.; Wang, S. C.; Ji, G. Application of metabolomics in traditional chinese medicine differentiation of deficiency and excess syndromes in patients with diabetes mellitus. *J. Evidence-Based Complementary Altern. Med.* **2012**, *2012*, 968083.
- (19) Menni, C.; Fauman, E.; Erte, I.; Perry, J. R.; Kastenmuller, G.; Shin, S. Y.; Petersen, A. K.; Hyde, C.; Psatha, M.; Ward, K. J.; Yuan, W.; Milburn, M.; Palmer, C. N.; Frayling, T. M.; Trimmer, J.; Bell, J. T.; Gieger, C.; Mohny, R. P.; Brosnan, M. J.; Suhre, K.; Soranzo, N.; Spector, T. D. Biomarkers for type 2 diabetes and impaired fasting glucose using a nontargeted metabolomics approach. *Diabetes* **2013**, *62* (12), 4270–4276.
- (20) Nikolic, S. B.; Sharman, J. E.; Adams, M. J.; Edwards, L. M. Metabolomics in hypertension. *J. Hypertens.* **2014**, *32* (6), 1159–1169.
- (21) Rodriguez-Gallego, E.; Guirro, M.; Riera-Borrull, M.; Hernandez-Aguilera, A.; Marine-Casado, R.; Fernandez-Arroyo, S.; Beltran-Debon, R.; Sabench, F.; Hernandez, M.; Del Castillo, D.; Menendez, J. A.; Camps, J.; Ras, R.; Arola, L.; Joven, J. Mapping of the circulating metabolome reveals alpha-ketoglutarate as a predictor of morbid obesity-associated non-alcoholic fatty liver disease. *Int. J. Obes.* **2014**, *2014*, 1–9.
- (22) Zhao, H.; Chen, J.; Shi, Q.; Ma, X.; Yang, Y.; Luo, L.; Guo, S.; Wang, Y.; Han, J.; Wang, W. Metabolomics-based study of clinical and animal plasma samples in coronary heart disease with blood stasis syndrome. *J. Evidence-Based Complementary Altern. Med.* **2012**, *2012*, 638723.
- (23) Vaarhorst, A. A.; Verhoeven, A.; Weller, C. M.; Bohringer, S.; Goral, S.; Meissner, A.; Deelder, A. M.; Henneman, P.; Gorgels, A. P.; van den Brandt, P. A.; Schouten, L. J.; van Greevenbroek, M. M.; Merry, A. H.; Verschuren, W. M.; van den Maagdenberg, A. M.; van Dijk, K. W.; Isaacs, A.; Boomsma, D.; Oostra, B. A.; van Duijn, C. M.; Jukema, J. W.; Boer, J. M.; Feskens, E.; Heijmans, B. T.; Slagboom, P. E. A metabolomic profile is associated with the risk of incident coronary heart disease. *Am. Heart J.* **2014**, *168* (1), 45–52.e7.
- (24) Jauhiainen, T.; Pilvi, T.; Cheng, Z. J.; Kautiainen, H.; Muller, D. N.; Vapaatalo, H.; Korpela, R.; Mervaala, E. Milk Products Containing Bioactive Tripeptides Have an Antihypertensive Effect in Double Transgenic Rats (dTGR) Harboring Human Renin and Human Angiotensinogen Genes. *J. Nutr. Metab.* **2010**, *2010*, 287030.
- (25) Guidelines Subcommittee. 1999 World Health Organization-International Society of Hypertension Guidelines for the Management of Hypertension. *J. Hypertens.* **1999**, *17* (2), 151–183.
- (26) Association, C. M. Guideline of nonalcoholic fatty liver disease diagnosis and therapy. *Zhonghua Ganzangbing Zazhi.* **2006**, *14* (3), 161–163.
- (27) Gibbons, R. J.; Chatterjee, K.; Daley, J.; Douglas, J. S.; Fihn, S. D.; Gardin, J. M.; Grunwald, M. A.; Levy, D.; Lytle, B. W.; O'Rourke, R. A.; Schafer, W. P.; Williams, S. V.; Ritchie, J. L.; Chaitlin, M. D.; Eagle, K. A.; Gardner, T. J.; Garson, A., Jr.; Russell, R. O.; Ryan, T. J.; Smith, S. C., Jr. ACC/AHA/ACP-ASIM guidelines for the management of patients with chronic stable angina: a report of the American College of Cardiology/American Heart Association Task Force on Practice Guidelines (Committee on Management of Patients With Chronic Stable Angina). *J. Am. Coll. Cardiol.* **1999**, *33* (7), 2092–2197.

- (28) Society of Cardiology, C. M. A. Editorial Committee of Chinese Journal of Cardiology. Diagnosis and treatment recommendation of unstable angina cordis. *Chin. J. Cardio.* **2000**, *28*, 409–412.
- (29) Xie, G.; Plumb, R.; Su, M.; Xu, Z.; Zhao, A.; Qiu, M.; Long, X.; Liu, Z.; Jia, W. Ultra-performance LC/TOF MS analysis of medicinal Panax herbs for metabolomic research. *J. Sep. Sci.* **2008**, *31* (6–7), 1015–1026.
- (30) Karnovsky, A.; Weymouth, T.; Hull, T.; Tarcea, V. G.; Scardoni, G.; Laudanna, C.; Sartor, M. A.; Stringer, K. A.; Jagadish, H. V.; Burant, C.; Athey, B.; Omenn, G. S. Metscape 2 bioinformatics tool for the analysis and visualization of metabolomics and gene expression data. *Bioinformatics* **2012**, *28* (3), 373–380.
- (31) Xia, J.; Wishart, D. S. MSEA: a web-based tool to identify biologically meaningful patterns in quantitative metabolomic data. *Nucleic Acids Res.* **2010**, *38* (suppl2), W71–W77.
- (32) Shannon, P.; Markiel, A.; Ozier, O.; Baliga, N. S.; Wang, J. T.; Ramage, D.; Amin, N.; Schwikowski, B.; Ideker, T. Cytoscape: a software environment for integrated models of biomolecular interaction networks. *Genome Res.* **2003**, *13* (11), 2498–2504.
- (33) Fischer, L. J.; Hamburger, S. A. Impaired insulin release after exposure of pancreatic islets to autooxidizing dihydroxyfumarate. *Endocrinology* **1981**, *108* (6), 2331–2335.
- (34) Delgado-Lista, J.; Perez-Martinez, P.; Lopez-Miranda, J.; Perez-Jimenez, F. Long chain omega-3 fatty acids and cardiovascular disease: a systematic review. *Br. J. Nutr.* **2012**, *107* (Suppl 2), S201–S213.
- (35) Nobili, V.; Carpino, G.; Alisi, A.; De Vito, R.; Franchitto, A.; Alpini, G.; Onori, P.; Gaudio, E. Role of docosahexaenoic acid treatment in improving liver histology in pediatric nonalcoholic fatty liver disease. *PLoS One* **2014**, *9* (2), e88005.
- (36) Depner, C. M.; Philbrick, K. A.; Jump, D. B. Docosahexaenoic acid attenuates hepatic inflammation, oxidative stress, and fibrosis without decreasing hepatosteatosis in a Ldlr(–/–) mouse model of western diet-induced nonalcoholic steatohepatitis. *J. Nutr.* **2013**, *143* (3), 315–323.
- (37) Rodrigues, A. F.; Roecker, R.; Junges, G. M.; de Lima, D. D.; da Cruz, J. G.; Wyse, A. T.; Dal Magro, D. D. Hypoxanthine induces oxidative stress in kidney of rats: protective effect of vitamins E plus C and allopurinol. *Cell Biochem. Funct.* **2014**, *32* (4), 387–394.
- (38) Dawson, J.; Walters, M. Uric acid and xanthine oxidase: future therapeutic targets in the prevention of cardiovascular disease? *Br. J. Clin. Pharmacol.* **2006**, *62* (6), 633–644.
- (39) Kerner, J.; Minkler, P. E.; Lesnfsky, E. J.; Hoppel, C. L. Fatty acid chain-elongation in perfused rat heart: synthesis of stearyl carnitine from perfused palmitate. *FEBS Lett.* **2007**, *581* (23), 4491–4494.
- (40) Koves, T. R.; Li, P.; An, J.; Akimoto, T.; Slentz, D.; Ilkayeva, O.; Dohm, G. L.; Yan, Z.; Newgard, C. B.; Muoio, D. M. Peroxisome proliferator-activated receptor-gamma co-activator 1alpha-mediated metabolic remodeling of skeletal myocytes mimics exercise training and reverses lipid-induced mitochondrial inefficiency. *J. Biol. Chem.* **2005**, *280* (39), 33588–33598.
- (41) Li, H.; Xu, M.; Lee, J.; He, C.; Xie, Z. Leucine supplementation increases SIRT1 expression and prevents mitochondrial dysfunction and metabolic disorders in high-fat diet-induced obese mice. *Am. J. Physiol.: Endocrinol. Metab.* **2012**, *303* (10), E1234–E1244.
- (42) Opara, E. C.; Petro, A.; Tevzian, A.; Feinglos, M. N.; Surwit, R. S. L-glutamine supplementation of a high fat diet reduces body weight and attenuates hyperglycemia and hyperinsulinemia in C57BL/6J mice. *J. Nutr.* **1996**, *126* (1), 273–279.
- (43) Shao, F.; Ford, D. A. Elaidic acid increases hepatic lipogenesis by mediating sterol regulatory element binding protein-1c activity in HuH-7 cells. *Lipids* **2014**, *49* (5), 403–413.
- (44) Chen, T.; Wong, Y. S. Selenocystine induces reactive oxygen species-mediated apoptosis in human cancer cells. *Biomed. Pharmacother.* **2009**, *63* (2), 105–113.
- (45) Baker, J. F.; Krishnan, E.; Chen, L.; Schumacher, H. R. Serum uric acid and cardiovascular disease: recent developments, and where do they leave us? *Am. J. Med.* **2005**, *118* (8), 816–826.
- (46) Kolentinis, M. K.; Verginadis, I. I.; Simos, Y. V.; Tsitou, N.; Karkabounas, S.; Kolettis, T. M.; Evangelou, A. M. Cardiovascular effects of vanillylmandelic acid in rats. *Eur. J. Pharmacol.* **2013**, *703* (1–3), 46–52.
- (47) Nogusa, Y.; Mizugaki, A.; Hirabayashi-Osada, Y.; Furuta, C.; Ohyama, K.; Suzuki, K.; Kobayashi, H. Combined Supplementation of Carbohydrate, Alanine, and Proline Is Effective in Maintaining Blood Glucose and Increasing Endurance Performance during Long-Term Exercise in Mice. *J. Nutr. Sci. Vitaminol.* **2014**, *60* (3), 188–193.
- (48) Connolly, G. P.; Duley, J. A. Uridine and its nucleotides: biological actions, therapeutic potentials. *Trends Pharmacol. Sci.* **1999**, *20* (5), 218–225.
- (49) Bramer, C. O.; Steinbuchel, A. The methylcitric acid pathway in *Ralstonia eutropha*: new genes identified involved in propionate metabolism. *Microbiology* **2001**, *147* (Pt 8), 2203–2214.
- (50) Cansev, M. Uridine and cytidine in the brain: their transport and utilization. *Brain Res. Rev.* **2006**, *52* (2), 389–397.
- (51) Dalazen, G. R.; Terra, M.; Jacques, C. E.; Coelho, J. G.; Freitas, R.; Mazzola, P. N.; Dutra-Filho, C. S. Pipecolic acid induces oxidative stress in vitro in cerebral cortex of young rats and the protective role of lipoic acid. *Metab. Brain Dis.* **2014**, *29* (1), 175–183.